Biochimica et Biophysica Acta, 1019 (1990) 73–80
Elsevier

BBABIO 43249

Mechanism of fatty acid effect on myocardial oxygen consumption. A phosphorus NMR study

Ilmo Hassinen [1], Kinji Ito [2,*], Shoko Nioka [3] and Britton Chance [2]

[1] Department of Medical Biochemistry, University of Oulu, Oulu (Finland) and Departments of [2] Biochemistry and Biophysics and [3] Physiology, School of Medicine, University of Pennsylvania, Philadelphia, PA (U.S.A.)

(Received 24 October 1989)

Key words: Energy state, cellular; Redox potential; Oxygen consumption; Hexanoate; NMR, ^{31}P-; (Isolated perfused rat heart)

The calorigenic effect of fatty acids on the intact myocardium was investigated in isolated rat hearts perfused with a phosphate-free bicarbonate buffer. ^{31}P-NMR spectra were accumulated in a Fourier transform high-field spectrometer during titration of the heart with varying concentrations of hexanoate. Oxygen consumption, coronary flow, left ventricular pressure development, heart rate and tissue surface fluorescence of nicotinamide-adenine nucleotides were monitored simultaneously. It was found that hexanoate within a range of 40 to 800 μM increased the reduction of NADH/NAD, increased oxygen consumption and increased the phosphocreatine/inorganic phosphate ratio in a concentration-dependent manner. The results suggest that the fatty acid-induced increase in oxygen consumption is not due to a primary effect on the cellular energy state resulting from a decrease in the P/O ratio or uncoupling of the mitochondria but due to an increase in the thermodynamic driving force.

Introduction

Fatty acids are the main fuel for the heart muscle in vivo [1], and it has been repeatedly observed that they increase the myocardial oxygen consumption as compared to carbohydrate oxidation [2]. This effect is of clinical importance for the myocardium when jeopardised due to underperfusion and hypoxia as a consequence of ischaemic heart disease. This fatty acid effect is not fully understood. It has been suggested that the increase in oxygen consumption may be due to the inherently lower P/O ratio for fatty acid oxidation. Oxygen consumption is 0.200 to 0.167 mol of O_2 per mol of ATP produced during the oxidation of fatty acids with chain lengths of C_2 to C_{16}, as contrasted to 0.158 mol O_2/mol ATP during the oxidation of glucose to CO_2. Fatty acids, particularly those with a long chain length also uncouple oxidative phosphorylation, but the mechanism of this effect is in dispute. It has been observed that this occurs in isolated mitochondria without any significant dissipation of the electrochemical potential difference of protons ($\Delta\tilde{\mu}_{H^+}$) across the inner membrane [3] under certain conditions, whereas under other conditions the membrane potential is decreased concomitantly with oxygen uptake stimulation in an oligomycin-sensitive manner [4]. Some results also point to intramitochondrial hydrolysis of fatty acyl-CoA, a reaction which in combination with the fatty acyl-CoA ligase constitutes an ATP-consuming cycle [4]. A fraction of the oxygen wasting effect of fatty acids on the myocardium remains during inhibition of their oxidation at the carnitine acyltransferase or thiolase steps [5], indicating that part of the effect is extramitochondrial or is not linked to β-oxidation.

If the primary effect of fatty acids on oxygen consumption were at the level of the cellular energy state, i.e. uncoupling, this could be detectable by measuring the phosphorylation state of the adenylates by ^{31}P-NMR. This method allows monitoring of consecutive periods of metabolic steady states in the same heart and can be combined with other non-invasive methods.

Materials and Methods

Chemicals. Hexanoic acid (grade puriss.) was obtained from Fluka AG, Buchs, Switzerland. The chem-

* Present address: Department of Cardiovascular Medicine, Hokkaido University, Sapporo, Japan.

Abbreviations: Cr, creatine; CrP, creatine phosphate; $E_{m7.4}$, standard oxidation-reduction potential at pH 7.4; ΔG, Gibbs' free energy change, P_i, inorganic phosphate; F, Faraday constant; R, gas constant; T, temperature in Kelvins; $M\dot{V}O_2$, myocardial oxygen consumption rate.

Correspondence: I. Hassinen, Department of Medical Biochemistry, University of Oulu, Kajaanintie 52 A, SF-90220 Oulu 22, Finland.

0005-2728/90/$03.50 © 1990 Elsevier Science Publishers B.V. (Biomedical Division)

icals for the perfusion buffers were obtained from Sigma Chemical Co., St. Louis, MO.

Animals and perfusion method. Male Sprague-Dawley rats weighing 355 ± 47 g (mean ± S.D.) were anaesthetised with intraperitoneal pentobarbital (100 mg/kg body weight), the heart was isolated and aortic perfusion by the Langendorff procedure installed. The perfusion fluid was a phosphate-free Krebs-Henseleit bicarbonate buffer [6] containing 10 mM glucose and in equilibrium with O_2/CO_2 (19 : 1). The pulmonary artery was cannulated and samples taken constantly by suction in order to prevent exposure of the effluent fluid to air. The aortic pressure was adjusted to 60 mmHg with an overflow head. Stock solutions of sodium hexanoate were injected at varying rates into the constant main flow of perfusate with an adjustable precision syringe pump. The tubings connecting the heart to the supportive perfusion equipment were thermostated to 37°C with a water mantle covering their whole length of 5 m.

Left ventricular pressure was monitored by a pressure transducer (Gould, Inc., Cupertino, CA) connected to a transmural Teflon catheter. Oxygen concentrations in the aortic and pulmonary arterial perfusate were monitored by miniature Clark electrodes (MI-730, Microelectrodes, Inc., Londonderry, NH) connected to a dual oxygen monitor (University of Pennsylvania Biomedical Instrumentation Group, Philadelphia, PA.). Coronary flow was measured by collecting the combined effluents from the pulmonary artery drain and the NMR tube outflow.

Optical methods. NADH (+ NADPH) fluorescence of the heart muscle was monitored with a surface fluorometer [7], the optical connection being made by means of a bifurcated fiber-optic light guide 5 m in length and 2.5 mm in diameter. A corrected fluorescence signal was obtained by subtracting from the actual fluorescence signal an appropriate fraction of the 366 nm excitation light reflected from the tissue, in this case in a 1 : 1 ratio [8]. The light guide was inserted into the left ventricle through the atrium and the endocardial fluorescence measured.

The experimental setup allowed calibration of the NADH fluorescence changes by reference to the basal level during glucose oxidation and to the anoxia achieved by global ischaemia imposed by stopping the aortic perfusion. For transforming the data to a form more suitable for quantitative evaluation, the fluorescence changes were converted to a free mitochondrial NADH/NAD ratio. For this purpose the principles first analysed by Bücher and co-workers [11] for the case of the cytosolic NADH/NAD ratio were used. Briefly, the NADH (and flavin) fluorescence changes (ΔF) in the myocardium have been previously demonstrated to correlate with changes in the mitochondrial (but not cytosolic) free NADH/NAD ratio, and that the correlation can be linearised by a plot of $1/\Delta F$ versus $1/\Delta([NADH]_f/[NAD]_f)$ [12]. This plot was constructed from the published fluorescence and mitochondrial $[NADH]_f/[NAD]_f$ values for rat hearts perfused under similar conditions in the presence of glucose and hexanoate [10,12]. The plot was used to transform the present data of fluorescence changes to mitochondrial free NADH/NAD ratios. For further evaluation, the NADH/NAD ratio was converted to the redox potential of the NAD(H) couple (E_hNAD) and to the free energy change in the reduction of oxygen by NADH (ΔG_{or}). $E_{m7.4}$ values of −336 mV for NAD(H) at 37° [13] and +805 mV for O_2 (at 0.2 atm) [14] were used in the calculations according to Eqns. 1 and 2:

$$E_h\text{NAD} = E_{m7.4} + (RT/2F) \cdot \ln\{[\text{NAD}]_f/[\text{NADH}]_f\} \quad (1)$$

and

$$\Delta G_{or} = -2F \cdot (E_hO_2 - E_h\text{NAD}) \quad (2)$$

Nuclear magnetic resonance. The ^{31}P-NMR spectra were recorded on a Bruker 500 pulsed Fourier transform NMR spectrometer equipped with a superconducting magnet having a field strength of 11.8 T (phosphorus frequency 202.46 MHz). The heart was placed in a 16 mm diameter NMR sample tube which was inserted into a laboratory-built phosphorus probe designed for small, isolated tissue volumes. The field was shimmed by using a phantom of the approximate dimensions of a rat heart and containing phosphate solution in water. A 0.03-ppm line width of the water proton resonance peak was obtained.

The spectra were accumulated using a pulse width of 40 μs, resulting in a 60° tilting angle, a pulse interval of 3.6 s and an acquisition time of 0.2 s. A line broadening of 40 Hz was imposed. The saturation factor was determined by measuring control spectra at 10-s pulse intervals and the same pulse width of 40 μs. No saturation was observed with the 3.6 s repetition rate. Two 8-min sets of 128 spectra were collected for each metabolic steady state of 16 min. The results were presented as averages of 128 spectra.

Statistical treatment of the data. Student's *t*-test for paired data was used to compare the mean values. Multiple regression analysis of all data points was used for the evaluation of correlations by implementing the Statgraphics program package (STSC, Inc., Rockville, MD) which also uses the *t*-test for evaluating the statistical significance of the regression coefficients obtained.

Results and Discussion

Oxygen consumption

Oxygen consumption increased in a concentration dependent manner when the hexanoate concentration was increased from zero to 2 mM. The increase in

$M\dot{V}O_2$ at the highest concentration used amounted to 34%. Since the theoretical oxygen consumption during hexanoate oxidation is 0.182 mol O_2 per mol ATP obtained, which is only 15% higher than during glucose oxidation (0.158), the oxygen consumption observed here cannot be explained solely by the increase in this O_2/ATP ratio.

Cellular redox state

Cellular redox state changes were monitored by NAD(P)H fluorometry of the intact tissue. Although nicotinamide nucleotides occur in most intracellular compartments, it has been shown that the reduced nicotinamide nucleotide fluorescence in the myocardium originates from the mitochondria and reflects the redox state of the free NADH pool of the mitochondrial matrix [9,10]. The fluorescence data were converted to the mitochondrial free NADH/NAD ratio as described in the Materials and Methods section. A summary of the redox state data is presented in Table I which shows that hexanoate caused mitochondrial NAD reduction in a concentration-dependent manner.

Cellular energy state

As shown by Chance and co-workers [15], the CrP/P_i ratio measured by ^{31}P-NMR can be used as a convenient signal of the cellular energy state. The ATP + ADP concentration in physiological metabolic states is approximately constant and because of the near equilibrium of the creatine kinase reaction in the myocardium [16], the CrP + P_i concentration is constant.

One way of estimating the $[ATP]_f/[ADP]_f \cdot [P_i]_f$ ratio is to combine the NMR data with biochemical determinations. This is needed because creatine is not visible in ^{31}P-NMR. The CrP + Cr concentration in the cytosol was here taken to be 20.1 mM [17, 18]. The area under the NMR peaks of CrP and P_i were converted to cytosolic concentrations by reference to the β-phosphorus peak of ATP, cytosolic concentration of which was taken to be 5.55 mM. These data can be inserted to Eqn. 3:

$$[ATP]_f/[ADP]_f \cdot [P_i]_f = K_{eq} \cdot [CrP] \cdot [H^+] / \{([Cr_T] - [CrP]) \cdot [P_i]\} \quad (3)$$

where the subscripts f and T refer to free and total concentrations, respectively, and K_{eq} is the equilibrium constant of the creatine kinase reaction ($2 \cdot 10^9$ M^{-1} at a $[Mg^{2+}]_f$ of 1.5 mM) [19]. Cytosolic $[H^+]$ was calculated from the equation:

$$[H^+] = 10^{-\{6.77 + \log[(\delta P_i - 3.29)/(5.68 - \delta P_i)]\}} M \quad (4)$$

where δP_i is the chemical shift (in ppm) of inorganic phosphate by reference to CrP [20]. The free energy change involved in ATP hydrolysis was further calculated from the equation:

$$\Delta G°_{ATP} = \Delta G_{ATP} + RT \cdot \ln\{[ADP]_f \cdot [P_i]_f/[ATP]_f\} \quad (5)$$

where $\Delta G°_{ATP} = -31.9$ kJ/mol under physiological conditions [21].

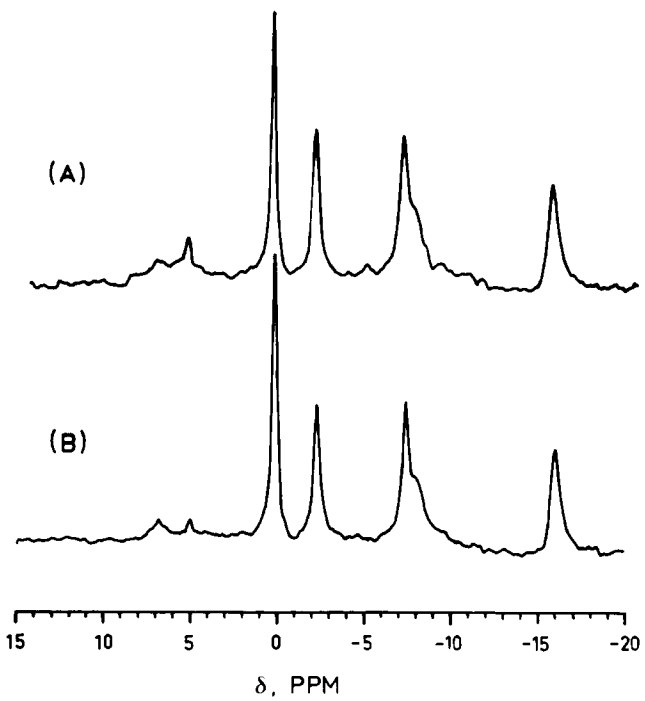

Fig. 1. ^{31}P-NMR spectra of an isolated rat heart perfused (A) under basal conditions (10 mM glucose as the only exogenous fuel) and (B) in the presence of 200 μM hexanoate. Each spectrum is constructed from the average of 128 free induction decays. 40-Hz line broadening was used. The peak assignments are: P_i, 5.0 ppm; CrP, 0 ppm; τ-ATP, −2.4 ppm; α-ATP, −7.4 ppm; β-ATP, −16.1 ppm.

An alternative procedure avoids recourse to parameters not measurable by ^{31}P-NMR by taking P_i/CrP as an indicator of $[ADP]_f$ (for the derivation of this principle, see ref. 15). This leads to the approximation that $[ATP]_f/[ADP]_f \cdot [P_i]_f$ is proportional to $[ATP]_f \cdot [CrP]_f/[P_i]^2$, and although P_i/CrP is not a linear function of $[ADP]_f$, the relation can be expected to hold within the range encountered physiologically. The data are shown in Table I.

Typical ^{31}P-NMR spectra under basal conditions and during the infusion of 200 μM hexanoate are presented in Fig. 1. The noise level permits reasonably accurate determination of P_i, which decreases to very low levels during fatty acid oxidation. The saturation error in CrP determination was below the level of detectability at the pulse repetition rate used.

As shown in Table I, the CrP/P_i ratio increased stepwise upon a corresponding increase of the perfusate hexanoate concentration to 0.8 mM. The change is equivalent to a doubling of the $[ATP]/[ADP] \cdot [P_i]$ ratio

TABLE I

Effect of hexanoate infusion on oxygen consumption, work output, free [NADH] / [NAD], [CrP] / [P_i], [ATP] / [ADP] · [P_i] and [ATP] · [CrP] / [P_i]^2 ratios and the free energy change involved in the mitochondrial NADH oxidation by oxygen and the cytosolic hydrolysis of ATP in the isolated perfused rat heart [a]

Parameter	Hexanoate concentration (μM)						
	0 (control) ($n = 8$) [b]	80 ($n = 6$)	200 ($n = 7$)	400 ($n = 6$)	800 ($n = 5$)	2000 ($n = 2$)	0 (recovery) ($n = 7$)
$M\dot{V}O_2$ (% initial)	100 ± 1	108 ± 3 *	121 ± 4 **	122 ± 5 **	127 ± 4 **	134 ± 4	106 ± 3
$\frac{[NADH]}{[NAD]}$ [c]	1.80 ± 0.00	1.93 ± 0.02 *	2.29 ± 0.05 **	2.55 ± 0.14 **	2.48 ± 0.08 ***	2.49 ± 0.00	1.81 ± 0.00
$\frac{[CrP]}{[P_i]}$ [d] (% initial)	100 ± 4	120 ± 13	151 ± 26 *	132 ± 14	151 ± 15 *	132 ± 11 **	83 ± 8
$\frac{[ATP]}{[ADP]\cdot[P_i]}$ [e] (10^3 M^{-1})	48.6 ± 3.8	57.3 ± 10.3	77.8 ± 15.1	64.6 ± 11.0	90.6 ± 16.0 *	83.6 ± 7.0 *	40.8 ± 4.6
$\frac{[ATP]\cdot[CrP]}{[P_i]^2}$ [f] (% of initial)	100 ± 9	146 ± 32	256 ± 97	184 ± 47	199 ± 35 *	162 ± 28 *	69 ± 13
ΔG_{or} [g] (kJ/2e$^-$)	−224.08 ± 0.0	−224.23 ± 0.04	−224.67 ± 0.08 ***	−224.94 ± 0.16 ***	−224.87 ± 0.10	−224.91 ± 0.00	−224.19 ± 0.10
ΔG_{ATP} (kJ/mol)	−59.65 ± 0.21	−59.94 ± 0.45	−60.70 ± 0.41	−60.30 ± 0.38	−61.17 ± 0.43 *	−61.11 ± 0.22	−59.17 ± 0.29
Rate · pressure product (% of initial)	100 ± 2	102 ± 6	100 ± 6	86 ± 6	90 ± 13	55 ± 0	97 ± 9

[a] Means ± S.E.
[b] Number of 8-min observation periods with 128 free induction decays in each. Data were accumulated from four hearts.
[c] Calculated from the NADH fluorescence change as described under Materials and Methods.
[d] The initial NMR peak area ratio was 3.8 ± 0.3.
[e] Calculated from the chemically determined tissue ATP and creatine concentrations and the CrP, P_i and β-ATP resonance peak areas in the NMR spectrum as described under Materials and Methods.
[f] The initial NMR peak area ratio was 12.2 ± 1.4.
[g] ΔG of oxidation of NADH by oxygen.
* $P < 0.05$, ** $P < 0.01$ and *** $P < 0.005$ as compared to controls.

or a 3% enhancement of the free energy change involved in ATP hydrolysis. It is significant that there was a lowering of the cellular energy state below the initial level after cessation of the fatty acid infusion, the reason for which could be a delay in the initiation of carbohydrate oxidation, which is almost completely suppressed during hexanoate oxidation [22] so that a temporary oxidation of the mitochondrial fluorescent flavins beyond the basal value is observed [23]. Oxidation was not so apparent in the present experiments.

It is noteworthy that the fatty acids did not appreciably affect the mechanical work output of the heart as evaluated from the peak intraventricular pressure-heart rate product (Table I).

Modelling and Statistics

Several theoretical frameworks have been proposed in the literature for describing quantitatively the regulation of cellular respiration. At least four approaches have been described: 1) classical enzyme kinetics [15], 2) the control theory of Kacser and Burns [24,25,26], 3) irreversible thermodynamics [27] and 4) the near-equilibrium hypothesis of Wilson and his co-workers [28,29].

Michaelis-Menten hyperbolic enzyme kinetics has been successfully applied recently to the quantitative description of in vivo ^{31}P-NMR data from skeletal muscle [15, 30].

The hyperbolic kinetics of the multisubstrate net reaction of oxidative phosphorylation (omitting the protons),

$$NADH_2 + 3\,ADP + 3\,P_i + \tfrac{1}{2}O_2 \rightarrow NAD + 3\,ATP + 4\,H_2O,$$

should obey the relation:

$$V/V_{max} = 1/\{1 + (K_1/[NADH_2]) + (K_2/[ADP]) + (K_3/[P_i]) + (K_4/[O_2])\}, \quad (6)$$

in which the constants K_1 to K_4 are the apparent Michaelis constants of the enzyme system for the substrates indicated in the same terms.

In the well oxygenated myocardium the O_2 concentration is kept almost constant due to coronary

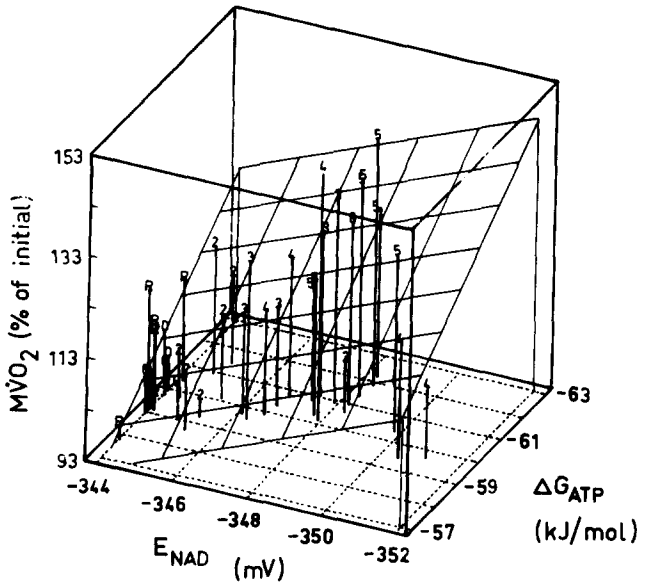

Fig. 2. Myocardial oxygen consumption as a function of the redox potential of the mitochondrial free NAD(H) system and the G of ATP hydrolysis in the cytosol. The experimental data and the response surface of a least squares fit of the data to a linear model are shown. The regression equation was $M\dot{V}O_2 + 2.91 \cdot E_h NAD + 5.43 \cdot G_{ATP} - 1273.7$. The experimental points are marked as: 0, zero controls; 2, 80 μM; 3, 200 μM; 4, 400 μM; 5, 800 μM, 6, 2000 μM hexanoate; R, return to zero.

autoregulation [31] and can be eliminated from the equation. To solve Eqn. 6 for the constants K_1 to K_3 by conventional regression analysis of the experimental data one has to obtain an estimate for V_{max}. This can be approximated from a linearization of a one-substrate Michaelis-Menten equation [15], e.g. the Hanes plot: $[S]/v$ versus [S], which yields V_{max} as the inverse of slope and $-K_m$ as the [S] axis intercept [32]. A Hanes' plot of $([NADH]/[NAD])/M\dot{V}O_2$ versus [NADH]/[NAD] for the data from the present isolated perfused heart gives a V_{max} value of 2.03 times the initial figure (Fig. 3). One should note that the plot is only used as a means of linearizing the data to provide an approximation for $M\dot{V}O_{2(max)}$, and not necessarily to describe the in vivo substrate affinity of NADH : ubiquinone oxidoreductase.

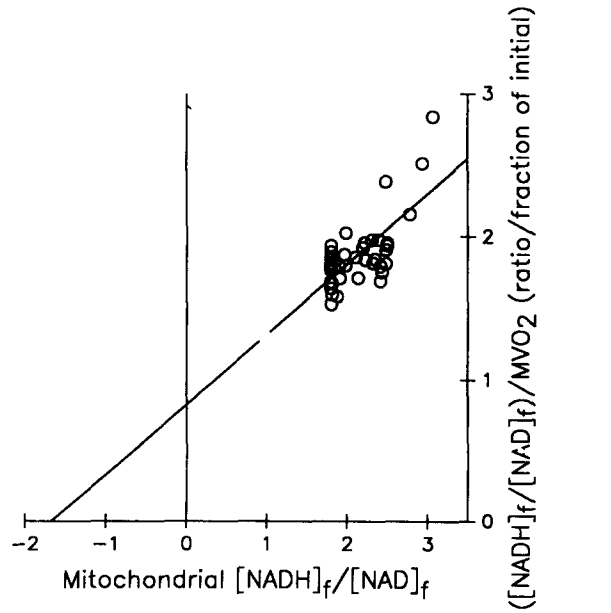

Fig. 3. Hanes plot of the myocardial oxygen consumption and the mitochondrial free NADH system. $[NADH]_f/[NAD]_f$ was used as the parameter reflecting $[NADH]_f$. The free NADH/NAD ratio was estimated as described under Materials and Methods.The least squares regression line is shown.

Once an estimate exists for V_{max}, the other constants of Eqn. 6 can be obtained by multiple regression of a set of data points, provided that there is not too much colinearity between the variables [33].

When the ^{31}P-NMR and redox data for hexanoate oxidation are fitted to Eqn. 6 using [NADH]/[NAD] to reflect $[NADH]_f$ and $[P_i]/[CrP]$ as an approximate indicator of $[ADP]_f$ [15], the equation takes the form:

$$M\dot{V}O_2 = 203.2/\{1 + 1.79/([NADH]/[NAD]) - 0.0048/([P_i]/[CrP]) + 0.46/[P_i]\}$$

where $M\dot{V}O_2$, $[P_i]/[CrP]$ and $[P_i]$ are expressed as % of initial values and the $M\dot{V}O_{2max}$ (203.2) is taken from the Hanes plot of Fig. 3.

Using these values for the proportionality constants as a starting point, the experimental data were fitted to the same equation by using an iterative nonlinear procedure employing the Marquardt algorithm [35]. This optimization gave Eqn 6. the form of

$$M\dot{V}O_2 = 183.2/\{1 + 1.43/([NADH]/[NAD] - 0.0043/([P_i]/[CrP]) + 0.40/[P_i]\}$$

with a correlation coefficient of 0.73. The further adjustments were rather small, indicating that the approximate V_{max} obtained from the Hanes plot is satisfactory.

Elimination of the negative term (K_2) and refeeding of the data points into the regression algorithm gives a negative value for the apparent K_m for P_i (K_3). Thus, stepwise selection of constants with positive values leaves only [NADH]/[NAD] in the model which takes the form

$$M\dot{V}O_2 = 183.2/(1 + 1.32/([NADH]/[NAD])), \quad (7)$$

upon which the fit to the model has a significance level of $P < 0.0001$.

The evident problem is that the redox state of the matrix free NADH/NAD couple shows the strongest controlling power in the case of fatty acid oxidation. Moreover, the fit to the Hanes plot (Fig. 3) deteriorates and gives a negative slope when the expression (NADH/NAD)/(1 + NADH/NAD) which has a lin-

ear relationship to $[NADH]_f$ is used as [S] in the Hanes plot. This means that the dependence of $M\dot{V}O_2$ on $[NADH]_f$ is too strong for a Michaelis-Menten relationship alone. Although the $[NADH]_f/[NAD]_f$ for the cytosol and mitochondrial matrix can be evaluated by means of appropriate indicator metabolites [10], the absolute free NADH concentration is difficult to estimate. It has been pointed out by Nioka and co-workers [36], however, that the physiological level of $[NADH]_f$ in the mitochondrial matrix is probably too high for any regulation of NADH : ubiquinone oxidoreductase by substrate availability.

In vitro experiments with mitochondria have yielded a $K_{m/app}$ of 20 μM for ADP [34] and this value together with the equilibrium constant of the creatine kinase reaction allow a $K_{m/app}$ of 0.6 to be estimated for P_i/CrP. This fits in with data from the skeletal muscle tested using an exercise protocol, i.e. by changing the energy consumption [30]. If this value is inserted into a Michaelis-Menten equation containing terms for P_i/CrP and NADH/NAD, the $K_{m/app}$ for NADH/NAD becomes 15, to fit with the mean values for these parameters under control conditions and during oxidation of 800 μM hexanoate (Table I). This is difficult to explain in terms of the in vitro properties of mitochondrial NADH:ubiquinone oxidoreductase, which has a K_m value of 15–133 μM for NADH, depending on the preparation and conditions [37], see also ref. 36.

One should also note that we are dealing with a special case of oxidation of a substrate with extraordinary reducing power, a fatty acid. Its reducing power on the myocardium can be demonstrated by the extensive reduction of flavoproteins, to almost the same degree as in anoxia [17]. The use of flavin fluorescence may not be straightforward in the case of fatty acids, however, because of the fluorescence of the flavins in the β-oxidation chain. The correlation between flavoprotein and NADH + NADPH fluorescence and the mitochondrial free NADH/NAD ratio in the isolated perfused heart was tested by Nuutinen and co-workers [12], who observed that 2 mM hexanoate +10 mM glucose caused a 78% reduction of the flavins and a 38% reduction of NAD compared with a substrate-free perfusion, detectable by surface fluorometry, when the response to anoxia was taken as 100%. This occurred concomitantly with an increase in the $[NADH_m]_f/[NAD_m]_f$ ratio from 0.82 to 4.1, as compared with 11.8 in anoxia [12].

The thermodynamic framework or oxygen concentration regulation involves the driving forces for the reactions. In non-equilibrium thermodynamics the reaction rate of oxidative phosphorylation is a linear function of the forces as in Eqn. 8:

$$J_{or} = -(L_{or} \cdot \Delta G_{or} + Lr_{ATP} \cdot \Delta G_{ATP}) \quad (8)$$

where L_{or} is the straight coefficient for the redox reaction, Lr_{ATP} is the cross coefficient for phosphorylation and J_{or} is the flux of the redox reaction.

According to the near-equilibrium hypothesis, a derivation based more on details of the reaction provides an oxygen consumption rate dependent on the mitochondrial [NADH]/[NAD] and $[ATP]/[ADP] \cdot [P_i]$ ratios [38].

When the data points are inserted into a linear equation:

$$M\dot{V}O_2 = a \cdot X + b \cdot Z + c,$$

in which X and Z are functions of the redox state of the NADH/NAD system and the cellular energy state, respectively, a good fit with the model is obtained when they are presented in terms of $-\Delta G_{or}$ and $-\Delta G_{ATP}$ (Table II and Fig. 2) or [NADH]/[NAD] and $[ATP]_f/[ADP]_f \cdot [P_i]_f$ calculated by means of Eqn. 3. (Table II.). Qualitatively similar results were obtained when $[ATP] \cdot [CrP]/[P_i]^2$ was used as an indicator of $[ATP]_f/[ADP]_f \cdot [P_i]_f$, although the maximum value for the energy state parameter shifted from that obtained at 2 mM to that at 200 μM hexanoate (Table I). This is probably due to the property of the $[ATP] \cdot [CrP]/[P_i]^2$ being more strongly dependent on $[P_i]$.

The findings are difficult to interpret in quantitative mechanistic terms because of the sign of the proportionality constant of the energy state parameter. The most probable explanation is that the primary determinant of oxygen consumption during fatty acid oxidation is the redox state of NAD(H) in the mitochondrial matrix. A shift in this parameter towards reduction increases the driving force of oxidative phosphorylation so that the ATP system becomes energised. This can also be anticipated on the basis of the near-equilibria at two of the energy conservation sites in the respiratory chain [28] which has been observed in the myocardium [17]. Regulation by the adenylate system may therefore be overridden by the driving force of the reaction. The present results clearly demonstrate that two separate but interconnected mechanisms of regulation of oxygen consumption operate in living cells, one based on cellular energy expenditure and the other on fuel availability and selection.

One should also note that under most physiological conditions, the redox potential of the substrate end of the respiratory chain is well regulated at a steady level and shows surprisingly small fluctuations during carbohydrate oxidation upon changes in cellular energy consumption, for example [17]. This is necessary for energy-linked regulation and is effected by the tightly regulated non-equilibrium reactions of carbohydrate metabolism, i.e. the phosphofructokinase and pyruvate dehydrogenase reactions [39]. It is significant that supranormal concentrations of pyruvate cause reduction of the mitochondrial NAD and a concomitant increase

TABLE II

Dependence of oxygen consumption on the redox state of mitochondrial free NAD(H) and the energization state of the adenylate system in the isolated perfused rat heart

Multiple linear regression analysis was performed by using data sets from 41 individual experimental points. Significance levels are given in parentheses.

Independent variable	Proportionality coefficient			
	regression equation with constant [a]		regression equation through origo [b]	
$[NADH_m]_f/[NAD_m]_f$	17.5	($P = 0.0004$)	47.5	($P < 0.0001$)
$[ATP]_f/[ADP]_f \cdot [P_i]_f$	0.0002	($P = 0.0005$)	0.000174	($P = 0.0375$)
Constant	64.3	($P < 0.0001$)	–	
$-\Delta G_{or}$	15.3	($P = 0.0005$)	−1.6	($P = 0.0006$)
$-\Delta G_{ATP}$	7.9	($P = 0.00008$)	8.0	($P < 0.0001$)
Constant	−3604.3	($P < 0.0001$)	–	
$[NADH_m]_f/[NAD_m]_f$	21.7	($P < 0.001$)	52.2	($P < 0.0001$)
$[ATP] \cdot [CrP]/[P_i]^2$	1.95	($P = 0.148$)	0.63	($P = 0.734$)
Constant	64.6	($P < 0.0001$)	–	

[a] Regression equation was of the general form of $y = a \cdot x + b \cdot z + c$, where x, y and z stand for the redox, oxygen consumption and energy-state parameter, respectively.

[b] Regression equation was of the general form of $y = a \cdot x + b \cdot z$, where x, y and z stand for the redox, oxygen consumption and energy-state parameter, respectively.

in oxygen consumption in isolated mitochondria [40]. The pyruvate effect on energy metabolism has recently been confirmed by using microcalorimetry of perifused papillary muscle by Daut and Elzinga [41], who attribute the effect to a decrease in inorganic phosphate, which is an inhibitor of the force production of the actomyosin ATPase. A P_i decrease was observed by Koretsky and Balaban [40] during pyruvate oxidation, and a similar change was found in the present experiments with hexanoate. No significant changes were observed in the mechanical work output in the present case, and also the direction of the change in the $[ATP]/[ADP] \cdot [P_i]$ ratio argues against the possibility that the fatty acid effect on oxygen consumption may be due to changes in contractile function. Fatty acids have been observed to increase oxygen consumption in other tissues such as the liver, but the direction and extent of the change in the ATP/ADP ratio is dependent on the presence of albumin [42], so that uncoupling may be one factor in these tissues.

The increasing driving force and the subsequent energization during fatty acid oxidation may be advantageous for the situations in which fatty acid mobilization usually occurs, typified by the release of alarm hormones. Under such conditions the metabolism of the heart muscle becomes regulated by peripheral tissues, namely by lipolysis.

The present data do not lend support to the view that uncoupling plays an important part in the "oxygen wasting" effect of fatty acids in intact tissues.

Acknowledgments:

This investigation was supported by the National Institutes of Health (U.S.A.) grant HL 18708 "Tissue Oxygen Gradients in Hypoxia and Hyperoxia" and grants from the Medical Research Council of the Academy of Finland and the Sigrid Juselius Foundation. We are indebted to Dr. A. Mayevsky for advice on using the fluorometric apparatus.

References

1 Rogers, W.J., Russe, R.D., McDaniel, H.G. and Rackley, C.E. (1977) Am. J. Cardiol. 40, 421–428.
2 Challoner, D.R. and Steinberg, D. (1966) Am. J. Physiol. 211, 897–902.
3 Rottenberg, H. and Hashimoto, K. (1986) Biochemistry 25, 1747–1755.
4 Schönfeld, P., Wojtczak, A.B., Geelen, M.J.H., Kunz, W. and Wojczak, L. (1988) Biochim. Biophys. Acta 936, 280–288.
5 Hütter, J.F., Piper, H.M. and Spieckermann, P.G. (1985) Am. J. Physiol. 249, 723–728.
6 Krebs, H.A. and Henseleit, K. (1932) Hoppe-Seylers Z. Physiol. Chem. 210, 33–36.
7 Mayevsky, A. and Chance, B. (1982) Science 217, 537–540.
8 Mayevsky, A., Zarchin, N. and Friedli, C.M. (1982) Brain Res. 236, 93–105.
9 Chapman, J.B. (1972) J. Gen. Physiol. 59, 135–154.
10 Nuutinen, E.M. (1984) Basic Res. Cardiol. 79, 49–58.
11 Bücher, T., Brauser, B., Conza, A., Klein, F., Langguth, O. and Sies, H. (1972) Eur. J. Biochem. 27, 301–317.
12 Nuutinen, E.M., Hiltunen, J.K., Hassinen, I.E. (1981) FEBS Lett. 128, 356–360.
13 Clark, M. (1960) Oxidation-reduction potentials of organic systems, pp. 489–490, Williams & Wilkins, Baltimore. .
14 Wood, P.M. (1987) Trends Biochem. Sci. 12, 250–251.
15 Chance, B., Clark, B.J., Nioka, S., Subramanian, H., Maris, J.M., Argow, Z. and Bode, H.(1985) Circulation 72, suppl. 4, 103–110.
16 Shoubridge, E.A., Jeffry, F.M., Keogh, J.M., Radda, G.K. and Seymour, A.M. (1985) Biochim. Biophys. Acta 847, 25–32.
17 Hassinen, I.E. and Hiltunen, K. (1975) Biochim. Biophys. Acta 408, 319–330.
18 Kiviluoma, K.T., Peuhkurinen, K.J. and Hassinen, I.E. (1986) J. Mol. Cell. Cardiol. 18, 1133–1142.

19 Noda, L., Kuby, S.A. and Lardy, H.A. (1954) J. Biol. Chem. 210, 83–95.
20 Vink, P., McIntosh, T.K. and Fader, A.I. (1988) Magn. Res. Med. 7, 95–99.
21 Guynn, R., and Veech, R.L. (1973) J. Biol. Chem. 248, 6966–6972.
22 Latipää, P.M., Peuhkurinen, K.J., Hiltunen, J.K. and Hassinen, I.E. (1985) J. Mol. Cell. Cardiol. 17, 1161–1171.
23 Latipää, P.M., Hiltunen, J.K., Peuhkurinen, K.J. and Hassinen, I.E. (1983) Biochim. Biochim. Acta 162–171.
24 Kacser, H. (1983) Biochem. Soc. Trans. 11, 35–40.
25 Kacser, H. and Burns, J.A. (1973) Symp. Soc. Exp. Biol. 32, 65–104.
26 Doussiere, J., Ligeti, E., Brandolin, G. and Vignais, V.P. (1984) Biochim. Biophys. Acta 766, 492–500.
27 Westerhoff, H.V., Hellingwerf, K.J., Arentz, J.C., Scholte, B.J. and Van Dam, K. (1981) Proc. Natl. Acad. Sci. USA 78, 3554–3558.
28 Wilson, D.F., Stubbs, M., Veech, R.L., Erecińska, M. and Krebs, H.A. (1974) Biochem. J. 140, 57–64.
29 Erecińska, M. and Wilson, D.F. (1982) J. Membr. Biol. 70, 1–14.
30 Chance, B., Leigh, J.S.Jr., Kent, J., McCully, K., Nioka, S., Clark, B.J., Maris, J.M. and Grahamn T. (1986) Proc. Natl. Acad. Sci. USA 83, 9458–9462.
31 Feigl. E.O. (1983) Physiol. Rev. 63, 1–205.
32 Hanes, C.S. (1932) Biochem. J. 26, 1406–1421.
33 Slinker, B.K. and Glantz, S.A. (1985) Am. J. Physiol. 249, R1-R12.
34 Chance, B. and Williams, G. (1955) J. Biol. Chem. 217, 383–393.
35 Marquardt, D.W. (1963) J. Soc. Industr. Appl. Math., 2, 431–441.
36 Nioka, S., Smith, D.S., Chance, B., Subramanian, H.V., Butler, S. and Karzenberg, M. (1989) Am. J. Physiol., in press.
37 Hatefi, Y. and Stermpel, K.E. (1969) J. Biol. Chem. 244, 2350-.
38 Owen, C.S. and Wilson, D.F. (1974) Arch. Biochem. Biophys. 161, 581–591.
39 Olson, M.S., Dennis, C.S., DeByusere, M.S. and Padma, A. (1978) J. Biol. Chem. 253, 7369–7375.
40 Koretsky, A.P. and Balaban, R.S. (1987) Biochim. Biophys. Acta 893, 398– 408.
41 Daut, J. and Elzinga, G. (1989) J. Physiol. (Lond.)413, 379–397.
42 Soboll, S., Grundel, S., Schwabe, U. and Scholz, R. (1984) Eur. J. Biochem. 141, 231–236.